Published in final edited form as:
Biomaterials. 2008 January ; 29(3): 327–336.

Construction and Characterization of a Thrombin Resistant Designer FGF-based-Collagen Binding Domain Angiogen

Brewster LP[1,2], **Washington C**[3], **Brey EM**[4,5], **Andrew Gassman**[1], **Subramanian A**[3], **Calceterra J**[3], **Wolf W**[4], **Hall CL**[5], **Velander WH**[3], **Burgess WH**[6], and **Greisler HP**[1,2,4,7,*]

1 *Loyola University Medical Center, Department of Surgery, 2160 South First Avenue, Maywood, IL, 60153*

2 *Loyola University Medical Center, Department of Cell Biology, Neurobiology, and Anatomy, 2160 South First Avenue, Maywood, IL, 60153*

3 *University of Nebraska, Department of Chemical and Biomolecular Engineering, Lincoln, NE, 68588*

4 *Edward J. Hines, Jr. VA Hospital, Research Services, 5th avenue & Roosevelt road, Hines, IL, 60141*

5 *Illinois Institute of Technology, Department of Biomedical Engineering, 10 West 32nd Street, Chicago, IL, 60616*

6 *StatSeal, Inc. Belleview, WA*

7 *Edward J. Hines, Jr. VA Hospital, Surgical Services, 5th avenue & Roosevelt road, Hines, IL, 60141*

Abstract

Humans demonstrate limited spontaneous endothelialisation of prosthetic bypass grafts. However the local application of growth factors to prosthetic grafts or to injured blood vessels can provide an immediate effect on endothelialisation. Novel chimeric proteins combining potent angiogens with extracellular matrix binding domains may localize to exposed matrices and provide sustained activity to promote endothelial regeneration after vascular interventions. We have ligated a thrombin-resistant mutant of FGF-1 (R136K) with a collagen binding domain (CBD) in order to direct this growth factor to sites of exposed vascular collagen or selected bioengineered scaffolds. While FGF-1 and R136K are readily attracted to a variety of matrix proteins, R136K-CBD demonstrated selective and avid binding to collagen ~4x that of FGF-1 or R136K alone ($P<.05$). The molecular stability of R136K-CBD was superior to FGF-1 and R136K. Its chemotactic activity was superior to R136K and FGF-1 (11%±1% vs. 6%±2% and 4%±1%; $P<.01$). Its angiogenic activity was similar to R136K and significantly greater than control by day 2 ($P<.01$). After day 3, FGF-1 treated ECs' sprouts had regressed back to levels insignificant compared to the control group ($P=.17$), while both R136K and R136K-CBD continued to demonstrate greater sprout lengthening as compared to control ($P<.0002$). The mitogenic activity of all growth factors was greater than control groups (20% PBS); in all comparisons ($P<.0001$). This dual functioning angiogen provides proof of concept for the application of designer angiogens to matrix binding proteins to intelligently promote endothelial regeneration of selected matrices.

*Corresponding Author: Howard P. Greisler, MD, Loyola University Medical Center, Department of Surgery, 2160 South First Avenue, Maywood, IL, 60153 708-216-8541; fax: 708-216-6300; hgreisl@lumc.edu.

Keywords

Angiogenesis; Collagen; Endothelial Cell; Endothelialisation; Fibroblast growth factor; Growth factors

1. Introduction

Cardiovascular interventions such as angioplasty or endarterectomy have the unintended effect of disrupting the target vessel's endothelium and disturbing its underlying internal elastic lamina [1,2]. Injury to the endothelium exposes the extracellular matrix (ECM) and results in thrombin deposition. This causes a chronically thrombogenic environment where platelets cluster and vascular smooth muscle cells (VSMC) transition to a synthetic phenotype, predisposing these vessels to thrombosis and myointimal hyperplasia [3–5]. Drug eluting stents deliver sustained local release of cytotoxic or antiproliferative drugs to the injured vessels; they have been shown to limit myointimal hyperplasia, but they also retard re-endothelialisation [6] and require prolonged anticoagulation to limit thrombotic complications [7,8]. Since injured vessels and bypass grafts have an intrinsically limited capacity to re-endothelialize after vascular interventions [9], therapeutic approaches that promote endothelialisation of injured vessels would likely lessen the frequency and magnitude of post-interventional complications [10]. Support for this idea has been demonstrated clinically by the superior long term patency rates of endothelial cell (EC) seeded prosthetic grafts compared to unseeded grafts [11,12].

The targeted delivery of EC-specific growth factors to injured vessels at the time of intervention could help to promote a rapid and complete re-endothelialisation [13,14]. Certain members of the fibroblast growth factor (FGF) family exhibit potent angiogenic activity that may be utilized as the basis for the design of molecular agents that promote endothelialisation [15–19]. FGF-1 in particular can promote endothelialisation of injured arteries and synthetic grafts [18,20, 21]. FGF-1 binds to four high-affinity FGF receptors and a low-affinity heparan sulfate proteoglycan receptor [22,23], leading to immediate ERK 1/2 phosphorylation (pMAPK 1 and 2), but mitosis requires sustained ERK activation for 4–8 hours through continuous exposure of FGF-1 to these receptors [24]; heparin and its analogues may augment this sustained activity in ECs [25–29].

We have engineered a thrombin-resistant mutant of FGF-1 through a lysine (K) for arginine (R) base substitution at residue 136 (termed R136K), the primary thrombin induced cleavage site, and demonstrated that R136K has superior chemotactic activity compared to FGF-1 on ECs in a thrombin rich environment while retaining FGF-1's mitogenic activity on ECs [30]. In the present study we ligate R136K to a collagen-binding domain (CBD) to generate R136K-CBD (Figure 1) in order to target this growth factor to collagen in order to increase its bioavailability and thereby chemotactic recruitment and proliferation of EC. Similar prototypes of growth factor-CBD have demonstrated mitogenic activity in vivo provided proof of concept for this approach. [31] Here we characterize R136K-CBD's ability to bind to collagen and direct endothelialisation via EC migration, proliferation, and angiogenesis.

2. Experimental Methods

2.1 Materials

Chemicals and biologicals were obtained as follows: oligonucleotide primers used for polymerase chain reaction (PCR) were purchased from Biosource International, Inc. (Camarillo, CA); Platinum PCR supermix, pCR2.1-TOPO® cloning vector, low melt agarose from Invitrogen Life Technologies (Carlsbad, CA); EcoRI, NdeI, Aat II, Bg I, II restriction endonucleases and Quick Ligase kit from New England Biolabs (Beverly, MA); Minelut Gel

Extraction kit from Qiagen, Inc. (Valencia, CA); Wizard Plus SV Miniprep kit from Promega Life Science (Madison, WI); pET 3C and Escherichia coli strain BL21 (pLysS) from Novagen (Madison, WI); heparin sepharose from Pharmacia Biotech (Piscataway, NJ); 0.05% trypsin/0.53 mM EDTA and collagenase from Gibco (Grand Island, NY); fibronectin, human thrombin, FGF-1 from the American Red Cross (Rockville, MD); thiopental sodium from Abbott Laboratories (Morris Plains, NJ); bovine lung heparin from Pharmacia and Upjohn (Kalamazoo, MI); anti-von Willebrand factor (vWF) antibody from Dako Corp (Carpenteria, CA); sodium dodecyl sulfate (SDS), activated MMP-2, and diethanolamine from Sigma Chemical Company (St. Louis, MO); tritiated thymidine from NEN Life Science Products (Boston, MA); methanol, trichloroacetic acid, acetic acid, sucrose, Tris-HCL, CaCl2, NaCl, and scintillation fluid from Fisher Scientific (Fair Lawn, NJ), Ultrafree-MC Centrifugal Filter Units from Millipore, Inc. (Billerica, MA), Collagenase A from Roche Diagnostics (Indianapolis, IN), insoluble type I collagen from Worthington (Lakewood, NJ), soluble type I collagen, and BIOCOAT Cell Culture Inserts from BD Biosciences (Bedford, MA), Gamma 5500B gamma counter and Z1 Beckman coulter counter from Beckman Coulter (Fullerton, CA), Eppendorf Centrifuge 5403 from Brinkmann Instruments (Westbury, NY), Human umbilical vein endothelial cells (HUVEC) from ATCC (Manassas, VA), BIACORE 3000 from Biacore, Inc. (Uppsala, Sweden), Tween 20 from J.T. Baker (Phillipsburg, NJ), and (KKK-H2N-[(Hyp)GP](8)KKK-OH) from New England Peptide, Inc. (Gardner, MA).

The media used were as follows: HUVEC growth medium (GM) consisted of EBM basal media, 10% FBS, and 0.1% gentamycin/amphotericin B; its quiescent media (QM) consisted of EBM basal media, 0.5% FBS, 5U/mL heparin, and 0.1% gentamycin/amphotericin B.

2.2 Construction and purification of the R136K-CBD chimera

The collagen binding domain (CBD) was provided by Professor Osamu Matsushita (Kagawa Medical Center). R136K was amplified to remove its stop codon with primers that introduced a NdeI (5′) and an EcoRI (3′) site. After PCR amplification and purification, this construct was ligated into the TOPO vector. Next the R136K and CBD were digested with restriction enzymes, ligated, and transformed into HB101 cells (Figure 1). Miniprep DNA purification was used on selected colonies, and positive clones were identified via restriction endonuclease mapping and DNA sequencing. The R136K-CBD Pet3c construct was then transformed into BL21 (pLysS) cells for expansion, induced with 50 nmol/L isopropyl thiogalactose, cultured for 16h at room temperature (RT) and 250 RPM, and the cells were collected by centrifugation (5000g). The cell pellet was thawed, resuspended in 100 mmol/L glucose, and the DNA was sheared by sonication. R136K-CBD was then purified by affinity-based chromatography using heparin sepharose chromatography and reversed phase HPLC. Its construction and purity were confirmed by SDS-PAGE and amino acid analysis.

2.3 Protein Iodination

FGF-1 and R136K-CBD were iodinated using Iodobeads according to instructions provided by the manufacturer (Pierce Chemical Co., Rockford, IL). Radioactivity was sampled in gamma counter, and sample integrity was verified by TCA precipitation and the concentrations were determined using the proteins' respective extinction coefficient at 280 nM absorbance.

2.4 Binding Assays

2.4.1 Iodinated R136K-CBD binding assays—In duplicate, Ultrafree-MC filters with 5mg of type I collagen were hydrated with 200 μL of collagen buffer (CB) (50mmol/L Tris-HCl, 5mmol/L CaCl2, 1.5 mol/L NaCl) at RT, centrifuged at 13,000g, and the filters were incubated with 0.1 mmol/L of ^{125}I-R136K-CBD in CB to a total volume of 60 μL. The filters were centrifuged at 13,000g again, and both the filters and filtrates were quantified as disintegrations per minute (DPMs) using a gamma counter (Beckman, Gamma 5500B). The

filters were then subsequently washed with 60 μL of PBS followed by increasing NaCl solutions (0.5–2.0 mol/L), centrifuged, and recounted in the gamma counter. Filters without collagen served as negative controls. To compare R136K-CBD's selectivity of binding to collagen, 5 mg collagen was incubated with either ^{125}I-R136K-CBD or ^{125}I-FGF-1, or ^{125}I-CBD or ^{125}I-R136K at 5nmol/L. Replicate samples of collagen with their native structure degraded until it was amorphous by collagenase A (0.1% w/v) prior to incubation with the iodinated growth factors were used to compare selectivity of this binding for intact collagen. The selectivity of binding to intact collagen type I was tested by dividing the bound growth factor radioactivity on intact collagen by the bound growth factor radioactivity on collagen that was degraded with collagenase, and the results were expressed in the following fashion: >100% represented selective binding to intact collagen; <100% represented selective binding to degraded collagen; =100% demonstrates no selectivity for either native or degraded collagen.

2.4.2 BIAcore activity assay—The affinity and binding kinetics of CBD, R136K and the R136K-CBD chimera were measured by surface plasmon resonance in a BIAcore-3000 (Molecular Interaction Facility, University of Nebraska Medical Center, Omaha, NE). A CM-1 chip was used in this particular study and the collagen binding peptide (P1) sequence is as follows: H2N-P(Hyp)GP(Hyp)GP(Hyp)GP(Hyp)GP(Hyp)GP(Hyp)GP(Hyp)GP(Hyp) GKKK-OH; this was immobilized on the CM-1 using N-hydroxysuccinimide-N-ethyl-N′-(dimethylaminopropyl)-carbodiimide chemistry as per manufacture's instructions. On an average, a residual resonance unit (RU) of 280 units was obtained after the immobilization of the peptide. All the analytes were diluted to a concentration in the range of 800 to 25 nm in HBS-E (10 mmol/L HEPES, 150 mmol/L NaCl, 3 mmol/L EDTA, pH 7.2) buffer containing 0.1 mg/ml of carboxymethyl dextran sodium salt. A pre-programmed method was used to run the samples on the BIAcore instrument. The association/disassociation constant was measured under continuous flow of 30 μl/min. All the resultant profiles were analyzed using the BIAevaluation™ software. All samples were assayed in duplicate and a minimum of five dilutions were run for each analyte. The equilibrium dissociation constant (K_d) was calculated as k_{off}/k_{on}.

2.5 Retention of Growth Factors and Proteolytic Resistance

2.5.1 Retention of growth factors in 3-D matrix—Equimolar (10nmol/L) amounts of ^{125}-I-R136K-CBD and ^{125}-I-FGF-1 were suspended in fibrin glue that was prepared as similarly described in 2-D [32] and incubated in GM. After 5 days of incubation the media and the fibrin glue's radioactivity were quantified as DPMs using a gamma counter (Beckman, Gamma 5500B).

2.5.2 Proteolytic resistance—The resistance to thrombin digestion was tested in vitro using 5μmol/L of FGF-1, R136K, or R136K-CBD suspended in 240μL of buffer solution with 2 U/mL thrombin at 37°C for serial time points, where 30 μL samples were collected (t=0, 4, 8, 24, and 30h). Proteins were then separated by SDS-PAGE electrophoresis, stained with Coumassie brilliant blue, and protein integrity was examined visually. Resistance to MMP-2 digestion used the above assay but substituting 200ng/mL of activated MMP-2 in place of thrombin.

2.6 R136K-CBDs Activity on ECs

2.6.1 Angiogenesis assay—Since regeneration of the endothelium can be induced through the addition of potent angiogens via biological matrices, we utilized our 3-dimensional angiogenesis assay [33], but modified it for human ECs. Here 2,250 HUVECs are incubated in 150 μL of media in nonadhesive plates to form a cell pellet. This pellet was then embedded in fibrin glue with 6 nmol/L FGF-1, R136K, or R136K-CBD and supported by a nylon mesh ring. The pellets were incubated in GM without exogenous growth factors, and the average

length of sprouts was determined by digital imagery (Scion Image software) at serial time points out to sprout stagnation (5 days). There were three replicate samples per treatment group, and the experiment was repeated twice with consistent results. The results are expressed as average length of sprout (μm) ± standard deviation.

2.6.2 EC migration assay—HUVEC migration was evaluated using a modified Boyden chamber that was pre-coated with type I collagen (BIOCOAT, BD Biosciences, Bedford, MA). 12,000 HUVECs were seeded into the upper well and then stimulated with 10nmol/L of soluble FGF-1, R136K, or R136K-CBD diluted in GM via the lower well. Replicate wells used these growth factors after thrombin incubation (2U/mL for 12 h). The plates were incubated for 4 h, and then the cells on the top and bottom of the insert membrane were trypsinized and counted in triplicate using a Z1 Beckman Coulter counter. There were three replicate wells per treatment group, and the experiment was repeated twice with similar results. Results are expressed as percent of migrating cells ± standard deviation.

2.6.3 EC proliferation assay—HUVEC or adult human dermal microvascular ECs (HDMECs) were plated onto 96-well type I collagen coated plates, grown to 80% confluence, quiesced by serum starvation in quiescence media (QM), then stimulated with either FGF-1, R136K, R136K-CBD, or CBD alone. 20% PBS was the negative control, and 20% fetal bovine serum (FBS) was the positive control. Proliferation was quantified by tritiated thymidine incorporation (1 μCi/well) using a scintillation counter (Packard, 2500TR). There were four replicate wells per treatment group, and all assays were repeated two times with similar results. All percentages are listed as percent positive control (20% FBS) ± standard deviation.

2.6.4 ERK 1/2 activation—Mitogen activation of ERK was quantified in ECs at selected time points after stimulation (2 minutes out to 24h) with 0.6 nmol/L R136K-CBD, R136K, or FGF-1 in QM. Again 20% PBS was the negative control, and 20% FBS was the positive control. After stimulation, the wells were washed with PBS and lysed with lysis buffer [34]. Cell lysates were sonicated, and the intracellular proteins collected after centrifugation. Protein concentration of the samples was determined using the BCA protein assay reagent kit (Pierce, Rockford, IL), and 10μg of each sample were subjected to SDS-PAGE prior to electrical transfer to nitrocellulose membranes. These membranes were probed with antibodies to ERK 1/2 (Santa Cruz Biotechnology; Santa Cruz, CA) and pMAPK (Promega, Madison, WI) at RT for 2h. Primary antibody binding was detected with horseradish peroxidase-conjugated (goat anti-rabbit) secondary antibody, and immunodetection was visualized by enhanced chemiluminescence (Amersham, Arlington Heights, IL). Densitometry was performed using UN-SCAN-IT™ software (Silk Scientific, Inc., Orem, UT), and the results were replicated at least twice with similar results.

2.7 Statistics

Normalized data (e.g. percent of positive or negative control, percent initial DPM) was used to compare the difference between treatment groups. At the level of alpha=0.05, a two-tailed Students t test (Excel Software, Microsoft, Redmond, WA) was used to determine significance between two groups; this level was corrected for multiple measures with an alpha=0.02 for comparison between three growth factors (FGF-1, R136K, and R136K-CBD).

3. Results

3.1 Binding of R136K-CBD to Collagen

Quantitative analysis of the equilibrium binding kinetics of R136K, R136K-CBD, or CBD towards a collagen mimetic surface having covalently immobilized (KKK-H2N-[(Hyp)GP](8) KKK-OH) was measured by surface plasmon resonance (BIAcore) analysis. Here both CBD

and R136K-CBD exhibited classical Langmuir binding behavior (Figure 2a,b) with similar values for their dissociation constant (K_d). This is in contrast to R136K (Figure 2c), which did not exhibit Langmuir model binding behavior. The residual binding units (RU) were as follows: a value of 111.46±19.22 was obtained for R136K-CBD; a value of 61.88± 1.96 was obtained for CBD alone, and a value of zero (indicating a lack of binding) was obtained with R136K. FGF-1's non-specific surface binding behavior along with its proclivity towards self-aggregation precluded its quantitative analysis by surface plasmon plasmon resonance.

3.2 Binding of R136K-CBD to type I collagen

Following incubation with collagen and after subsequent salt elutions, ^{125}I-R136K-CBD had significantly greater binding to 5mg collagen supported on a Millipore® filter than to these filters without collagen (P<.01) (Figure 3a). When comparing binding of ^{125}I-R136K-CBD and ^{125}I-FGF-1 to collagen supported on a Millipore® filter, ^{125}I-R136K-CBD demonstrated significantly greater binding than ^{125}I-FGF-1 after elution with 2 mol/L NaCl (46% +/− 4% vs. 33% +/−1%; P=.04). Selectivity was defined as the ratio of protein binding to collagen divided by the protein binding to collagenase-degraded collagen. This was utilized to demonstrate the selectivity of these growth factors for intact collagen as compared to its denatured matrix. Here, both ^{125}I-R136K-CBD and ^{125}I-CBD exhibited selectivity for collagen relative to collagenase-degraded collagen; ^{125}I-FGF-1 and ^{125}I-R136K did not. For example, ^{125}I-CBD exhibited a 2.5-fold increase in selectivity compared to R136K (257%±7% vs. 118%±8% at 2mol/L NaCl; P=.003). Similarly ^{125}I-R136K-CBD exhibited a 3.5-fold increase in selectivity compared to ^{125}I-FGF-1 (366%±36% versus 92%±5% at 2mol/L NaCl; P<.0001; Figure 3b).

3.3 Resistance to proteolytic degradation and retention in fibrin hydrogel

Protein molecular stability when exposed to thrombin and matrix metalloprotease-2 proteases was evaluated by SDS-PAGE at various exposure durations. R136K-CBD exhibited greater molecular stability out to 24 H after incubation with human thrombin (2U/mL) relative to both FGF-1 and R136K (Figure 4). R136K-CBD also demonstrated similar extended molecular stability after incubation with matrix metalloprotease-2 (data not shown). There was increased retention of radiolabeled R136K-CBD to FGF-1 within this fibrin gel formulation. Here more ^{125}I-R136K-CBD was retained in the fibrin gel as compared to ^{125}I-FGF-1 at the 5 day time point (46%±2% versus 14%±1%; P=.0001).

3.4 Angiogenic Activity

The angiogenic differentiation of HUVECs that were embedded in fibrin gel suspensions containing either R136K-CBD, R136K, FGF-1, or normal saline alone (untreated control) was monitored over a 5 day culture period (Figure 5). At day 2, R136K-CBD and R136K, but not FGF-1, stimulated greater lengths of EC sprouting than the untreated control group (R136K-CBD: 287μm±44μm, P=.007; R136K: 295μm±47μm, P=.005; FGF-1: 247μm±68μm, P=.14; control: 188μm±57μm). By day 3, all growth factor containing treatment groups showed differentiation that was greater than the untreated control (P<.0001). After day 3, FGF-1 treated ECs' sprouts had regressed back to levels insignificant compared to the control group (P=.17), while both R136K and R136K-CBD continued to demonstrate greater sprout lengthening as compared to control (P<.0002; Figure 5b). Sprout regression in R136K and R136K-CBD was not seen until day 6.

3.5 Chemotactic Activity

The chemotactic activity of these growth factors before and after treatment with thrombin was measured using a modified Boyden's chamber in which cells migrate through a collagen coated migration barrier. The percent relative migration response is defined as the percentage of cells

appearing on the lower side of the migration barrier. The relative migration response of growth factors was R136K-CBD>R136K (11%±1% vs. 6%±2%; P=.0001); R136K>FGF-1(6%±2% vs. 4%±1%; P=.009); and FGF-1 >growth media alone (4%±1% vs. 2%±1%; P=.01). After treatment of the growth factors with thrombin, the relative migration response of R136K-CBD and R136K was unchanged, but FGF-1 no longer demonstrated chemotactic activity compared to control (Figure 6).

3.6 Mitogenic Activity and ERK activation

The proliferative effect of FGF-1, R136K, and R136K-CBD on HUVECS and HDMECs during cell culture in vitro was measured. All of the growth factors exhibited heparin dependent mitogenic activity for both ECs. After serum starvation, R136K-CBD demonstrated robust mitogenic activity on HUVECs beginning at 0.6 nmol/L that was 109% ± 21% positive control (20% fetal bovine serum). This was comparable to that of R136K (103% ± 21%; P=.59) and FGF-1 (96% ± 13%;P=.16) respectively (Figure 7a). The proliferative response to all growth factor dosed treatment groups was greater than non-dosed treatment groups (20% PBS); (P<.0001 in all comparisons). R136K-CBD, R136K, and FGF-1 also demonstrated similar mitogenic activity on HDMECs at 0.6nmol/L (Figure 7b) that was significantly greater than in non-dosed negative control cultures (P<.0001 for all comparisons). Importantly, the iodinated forms of these proteins used in the above binding studies retained their mitogenic effects on ECs, while CBD itself elicited no mitogenic effect on ECs.

ERK-1 and ERK-2 activation (pMAPK 1 and 2) was measured as a corroborating indicator of mitogenesis signaling induced by these same cell culture treatment groups on HUVECs. Early activation was quantified at 2, 10, 20, and 60 minutes (Figure 7c,d). At all time points after stimulation with R136K-CBD, HUVECs had increased activation of ERK 1 and 2 (pERK 1 and pERK2) compared to that of the negative control (P<.020; Figure 7c, d). The basal ERK 1 and 2 expression were not different between groups at any time point (P>.2). When R136K-CBD's pMAPK 1 and 2 levels were compared to that of FGF-1 and R136K, both FGF-1 and R136K respectively, had ~1.5 to 2 fold greater pMAPK 1 and 2 activation than R136K-CBD that persisted at all time points but was not significant (P>.05). Since proliferation requires sustained ERK activation, we examined late pMAPK 1 and 2 activation at 6, 12, and 24h. Here the R136K-CBD treatment group had a sustained elevation of pMAPK 1 and 2 levels at 6 and 24h that was significantly greater than that of the negative control (P<.02). Again at these time points, there was ~1.5 fold increase in R136K and FGF-1 activation of ERK 1 and 2 compared to that of R136K-CBD, but again this increase was not significant (P>.05) for any comparisons (Figure 7e,f). Further basal ERK 1 and 2 expression were not significantly different between time points or treatment groups at any time point (P>.52).

4. Discussion

Recombinant derivatives of this CBD have been reported to bind to collagen and effect sustained activity by a variety of naturally occurring growth factors [35–38]. Such growth factors can be designed to exploit beneficial properties through focused mutations (here thrombin resistant activity) to intelligently direct endothelial regeneration [10,39]. Here we demonstrate that R136K-CBD improves upon or retains the angiogenic, chemotactic, and mitogenic advantage of R136K over FGF-1 and that the addition of R136K to the CBD does not negatively influence the selective binding activity of CBD.

Pragmatically, this selectivity may be utilized to bind R136K-CBD to exposed collagen in the extracellular matrix after endothelial injury or to bioengineered collagen matrices. This would provide delivery of the growth factor to where it is needed most (i.e. the injured vessel) and minimize the amount of growth factor that is released into the circulation or adsorbed non-specifically along uninjured portions of the vessel. R136K-CBD binding to type I collagen was

shown to have kinetics consistent with specific, high affinity binding sites as measured by surface plasmon resonance. In contrast R136K showed non-Langmuir adsorption behavior not consistent with structured and specific binding sites existing within collagen. R136K-CBD's dissociation binding constant (K_d) of 8×10^{-9} was comparable to that of CBD alone (Kd= 3×10^{-9}), indicating that the R136K-CBD collagen binding behavior is decidedly due to the presence of the CBD structure. Thus, we quantitatively have established that R136K-CBD would have an engineered propensity to create a depot of growth factor specifically at collagen surfaces, as opposed to reservoirs at non-collagenous surfaces (e.g. intact endothelium surrounding site of injury). This high affinity binding may result in the release of low growth factor concentrations near collagen surfaces with steeper local concentration gradients than what would be expected for R136K alone.

Importantly, our studies have shown that the addition of the CBD to R136K did not diminish R136K's thrombin resistance, rather it demonstrated superior molecular stability compared to FGF-1 in the presence of thrombin and MMP-2. This may be exploited in order to sustain the beneficial effects of R136K-CBD during the thrombogenic reaction to vascular interventions [40]. Increased proteolytic stability of R136K-CBD in combination with selective collagen binding conferred by the CBD would be expected to enhance and prolong growth factor depot effects upon chemotactic and angiogenic activity for ECs; this effect was seen relative to FGF-1 and R136K. As expected R136K retained its chemotactic activity after incubation with thrombin, however FGF-1 lost its chemotactic activity when exposed to thrombin. While a prolongation of chemotactic activity was expected with R136K-CBD and R136K, the impact of lower bulk concentrations as well as steeper concentration gradients near the collagen surface due to the high affinity binding of the chimera was not predictable. The greater chemotactic activity observed for R136K-CBD through a collagen-coated diffusion barrier relative to R136K implies that chemotaxis of ECs may be more efficiently driven by steep local concentration gradients rather than by higher bulk concentrations that would appear for the more soluble R136K.

R136K-CBD demonstrated similar mitogenic activity on ECs compared to FGF-1 and R136K; this activity correlated with an early and persistent increase in pMAPK 1 and 2 activation over 24h. Suprisingly pMAPK levels were less than that stimulated by FGF-1 and R136K. This may be due in part to peculiarities of FGF-1 signaling, in that sustained ERK 1/2 activation and cell cycle progression requires the internalization of FGF-1 or a truncated portion of it [41]. This internalization begins quickly after FGF-1 exposure with ½ of exogenous FGF-1 internalized within the cytosol by 30 minutes; this is reported to be necessary for the later signaling events required for cell proliferation [41,42], but the exact nature of the relationship between the internalization of FGF-1 and sustained ERK activation remains unclear. The 24kDa CBD may limit the degree or retard the efficiency of R136K-CBD internalization (or the cytosolic proteolytic processing involved in this process). However, since the angiogenic, chemotactic, and mitogenic activities of R136K-CBD were not diminished compared to FGF-1 or R136K, the practical importance of this relative decrease in pMAPK 1 and 2 is not known. Further although sustained ERK activation is a requirement of cell proliferation, its importance in cell migration or angiogenesis is not known. Since both chemotaxis and angiogenic sprouting are evident in a short time period (4h in this study for cell migration), sustained ERK activation (or other the late signaling events promulgated by FGF-1 internalization) do not seem to be necessary for these cellular activities; thus, even if R136K-CBD internalization is limited, it may have no effect on its chemotactic and angiogenic activity.

Angiogenesis has a particularly important role in the endothelialisation of injured arteries or synthetic grafts because it can promote endothelialisation via angiogenic induction from the adventitial vasculature (vasa vasorum) or from that of the tissue surrounding synthetic grafts. This can occur at multiple points circumferentially along the length of a non-endothelialized

artery, after angioplasty or operation, or bypass grafts after implantation. [43] This is because the radial distance for capillary induction from the adventitia toward the lumen is biologically compatible with EC behavior (μm), whereas the considerable lengths necessary for coverage with ECs via migration and proliferation from the edge of injury is not (cm-m) [44,45]. The sustained angiogenic response of R136K-CBD in our 3-D fibrin gel was due in part to resistance to thrombin proteolysis (R136K) as well as increased retention in the gel secondary to its increased size (43kDa compared to 17kDa). For this reason R136K-CBD is particularly exciting for application in vivo to regenerate endothelium in injured vessels and for promoting endothelialization of selected biomatrices.

To date we have been able to promote re-endothelialisation *in vivo* by suspending growth factors within a fibrin gel matrix for localized delivery to injured vessels and synthetic grafts [39,46]. Unfortunately since fibrin gel is comprised of thrombin and fibrinogen, which are both bioactive materials, this delivery system may have unintended effects that could hypothetically contribute to myointimal hyperplasia [47,48]. However R136K has demonstrated EC-specific chemotactic activity through a modified Boyden chamber with a fibrin gel barrier [30]. By ligating R136K to the ECM-binding CBD, we circumvent the necessity of a delivery vehicle such as fibrin gel for R136K, lessen the complexity of the delivery system, and allow better control of the variables of growth factor delivery.

5. Conclusion

This work demonstrates that R136K-CBD has many of the intended beneficial characteristics of its design, including both avid and selective binding to collagen and potent angiogenic, mitogenic and chemotactic activity for ECs. These qualities may be useful in promoting vascular regeneration of injured arteries or endothelialisation of selected collagen-based bioengineering scaffolds.

Acknowledgements

Supported by grants from the NIH R01-HL41272 (HPG), HL078151-01 (LPB), HL074594 (EMB) and Department of Veteran's Affairs (HPG, EMB).

References

1. Parikh SA, Edelman ER. Endothelial cell delivery for cardiovascular therapy. Adv Drug Deliv Rev 2000;42:139–161. [PubMed: 10942819]
2. Serruys PW, Kutryk MJ, Ong AT. Coronary-artery stents. N Engl J Med 2006;354:483–495. [PubMed: 16452560]
3. Schwartz SM. The intima: A new soil. Circ Res 1999;85:877–879. [PubMed: 10559132]
4. Schwartz SM, deBlois D, O'Brien ER. The intima. Soil for atherosclerosis and restenosis. Circ Res 1995;77:445–465. [PubMed: 7641318]
5. Clowes AW, Kirkman TR, Clowes MM. Mechanisms of arterial graft failure. II. Chronic endothelial and smooth muscle cell proliferation in healing polytetrafluoroethylene prostheses. J Vasc Surg 1986;3:877–884. [PubMed: 3712635]
6. Oyabu J, Ueda Y, Ogasawara N, Okada K, Hirayama A, Kodama K. Angioscopic evaluation of neointima coverage: sirolimus drug-eluting stent versus bare metal stent. Am Heart J 2006;152:1168–1174. [PubMed: 17161071]
7. Bavry AA, Kumbhani DJ, Helton TJ, Borek PP, Mood GR, Bhatt DL. Late thrombosis of drug-eluting stents: a meta-analysis of randomized clinical trials. Am J Med 2006;119:1056–1061. [PubMed: 17145250]
8. Pfisterer M, Brunner-La Rocca HP, Buser PT, Rickenbacher P, Hunziker P, Mueller C, et al. Late clinical events after clopidogrel discontinuation may limit the benefit of drug-eluting stents: an observational study of drug-eluting versus bare-metal stents. J Am Coll Cardiol 2006;48:2584–2591. [PubMed: 17174201]

9. Kraiss, L.; Clowes, A. Response of the arterial wall to injury and intimal hyperplasia. In: Sidawy, A.; Sumpio, B.; Depalma, R., editors. The Basic Science of Vascular Disease. Futura Publishing Company, Inc; Armonk, NY: 1997. p. 289
10. Brewster LP, Brey EM, Greisler HP. Cardiovascular gene delivery: The good road is awaiting. Adv Drug Deliv Rev 2006;58:604–629. [PubMed: 16769148]
11. Meinhart JG, Deutsch M, Fischlein T, Howanietz N, Froschl A, Zilla P. Clinical autologous in vitro endothelialization of 153 infrainguinal ePTFE grafts. Ann Thorac Surg 2001;71:S327–331. [PubMed: 11388216]
12. Deutsch M, Meinhart J, Fischlein T, Preiss P, Zilla P. Clinical autologous in vitro endothelialization of infrainguinal ePTFE grafts in 100 patients: a 9-year experience. Surgery 1999;126:847–855. [PubMed: 10568184]
13. Folkman J. How the field of controlled-release technology began, and its central role in the development of angiogenesis research. Biomaterials 1990;11:615–618. [PubMed: 1708683]
14. Greisler HP, Gosselin C, Ren D, Kang SS, Kim DU. Biointeractive polymers and tissue engineered blood vessels. Biomaterials 1996;17:329–336. [PubMed: 8745330]
15. Malecki J, Wesche J, Skjerpen CS, Wiedlocha A, Olsnes S. Translocation of FGF-1 and FGF-2 across vesicular membranes occurs during G1-phase by a common mechanism. Mol Biol Cell 2004;15:801–814. [PubMed: 14657241]
16. Sellke FW, Li J, Stamler A, Lopez JJ, Thomas KA, Simons M. Angiogenesis induced by acidic fibroblast growth factor as an alternative method of revascularization for chronic myocardial ischemia. Surgery 1996;120:182–188. [PubMed: 8751581]
17. van der Bas JM, Quax PH, van den Berg AC, van Hinsbergh VW, van Bockel JH. Ingrowth of aorta vascular cells into basic fibroblast growth factor-impregnated vascular prosthesis material: a porcine and human in vitro study on blood vessel prosthesis healing. J Vasc Surg 2002;36:1237–1247. [PubMed: 12469057]
18. Bjornsson TD, Dryjski M, Tluczek J, Mennie R, Ronan J, Mellin TN, et al. Acidic fibroblast growth factor promotes vascular repair. Proc Natl Acad Sci U S A 1991;88:8651–8655. [PubMed: 1717983]
19. Burgess WH, Mehlman T, Marshak DR, Fraser BA, Maciag T. Structural evidence that endothelial cell growth factor beta is the precursor of both endothelial cell growth factor alpha and acidic fibroblast growth factor. Proc Natl Acad Sci U S A 1986;83:7216–7220. [PubMed: 3532107]
20. Gray JL, Kang SS, Zenni GC, Kim DU, Kim PI, Burgess WH, et al. FGF-1 affixation stimulates ePTFE endothelialization without intimal hyperplasia. J Surg Res 1994;57:596–612. [PubMed: 7526046]
21. Zarge JI, Huang P, Husak V, Kim DU, Haudenschild CC, Nord RM, et al. Fibrin glue containing fibroblast growth factor type 1 and heparin with autologous endothelial cells reduces intimal hyperplasia in a canine carotid artery balloon injury model. J Vasc Surg 1997;25:840–848. [PubMed: 9152311]discussion 848–849
22. Prudovsky I, Savion N, Zhan X, Friesel R, Xu J, Hou J, et al. Intact and functional fibroblast growth factor (FGF) receptor-1 trafficks near the nucleus in response to FGF-1. J Biol Chem 1994;269:31720–31724. [PubMed: 7527394]
23. Maciag T, Friesel RE. Molecular mechanisms of fibroblast growth factor-1 traffick, signaling and release. Thromb Haemost 1995;74:411–414. [PubMed: 8578497]
24. Zhan X, Hu X, Friesel R, Maciag T. Long term growth factor exposure and differential tyrosine phosphorylation are required for DNA synthesis in BALB/c 3T3 cells. J Biol Chem 1993;268:9611–9620. [PubMed: 7683656]
25. Donohue PJ, Hsu DK, Guo Y, Burgess WH, Winkles JA. Fibroblast growth factor-1 induction of delayed-early mRNA expression in NIH 3T3 cells is prolonged by heparin addition. Exp Cell Res 1997;234:139–146. [PubMed: 9223379]
26. Terranova VP, DiFlorio R, Lyall RM, Hic S, Friesel R, Maciag T. Human endothelial cells are chemotactic to endothelial cell growth factor and heparin. J Cell Biol 1985;101:2330–2334. [PubMed: 3905825]
27. Barzu T, Lormeau JC, Petitou M, Michelson S, Choay J. Heparin-derived oligosaccharides: affinity for acidic fibroblast growth factor and effect on its growth-promoting activity for human endothelial cells. J Cell Physiol 1989;140:538–548. [PubMed: 2550475]

28. Burgess WH, Shaheen AM, Hampton B, Donohue PJ, Winkles JA. Structure-function studies of heparin-binding (acidic fibroblast) growth factor-1 using site-directed mutagenesis. J Cell Biochem 1991;45:131–138. [PubMed: 1711526]
29. Mueller SN, Thomas KA, Di Salvo J, Levine EM. Stabilization by heparin of acidic fibroblast growth factor mitogenicity for human endothelial cells in vitro. J Cell Physiol 1989;140:439–448. [PubMed: 2777882]
30. Erzurum VZ, Bian JF, Husak VA, Ellinger J, Xue L, Burgess WH, et al. R136K fibroblast growth factor-1 mutant induces heparin-independent migration of endothelial cells through fibrin glue. J Vasc Surg 2003;37:1075–1081. [PubMed: 12756357]
31. Nishi N, Matsushita O, Yuube K, Miyanaka H, Okabe A, Wada F. Collagen-binding growth factors: production and characterization of functional fusion proteins having a collagen-binding domain. Proc Natl Acad Sci U S A 1998;95:7018–7023. [PubMed: 9618531]
32. Shireman PK, Hampton B, Burgess WH, Greisler HP. Modulation of vascular cell growth kinetics by local cytokine delivery from fibrin glue suspensions. J Vasc Surg 1999;29:852–861. [PubMed: 10231637]discussion 862
33. Xue L, Greisler HP. Angiogenic effect of fibroblast growth factor-1 and vascular endothelial growth factor and their synergism in a novel in vitro quantitative fibrin-based 3-dimensional angiogenesis system. Surgery 2002;132:259–267. [PubMed: 12219021]
34. Schlaepfer DD, Hunter T. Evidence for in vivo phosphorylation of the Grb2 SH2-domain binding site on focal adhesion kinase by Src-family protein-tyrosine kinases. Mol Cell Biol 1996;16:5623–5633. [PubMed: 8816475]
35. Matsushita O, Jung CM, Minami J, Katayama S, Nishi N, Okabe A. A study of the collagen-binding domain of a 116-kDa Clostridium histolyticum collagenase. J Biol Chem 1998;273:3643–3648. [PubMed: 9452493]
36. Ishikawa T, Terai H, Kitajima T. Production of a biologically active epidermal growth factor fusion protein with high collagen affinity. J Biochem (Tokyo) 2001;129:627–633. [PubMed: 11275564]
37. Kitajima T, Terai H, Ito Y. A fusion protein of hepatocyte growth factor for immobilization to collagen. Biomaterials 2007;28:1989–1997. [PubMed: 17239947]
38. Lin H, Chen B, Sun W, Zhao W, Zhao Y, Dai J. The effect of collagen-targeting platelet-derived growth factor on cellularization and vascularization of collagen scaffolds. Biomaterials 2006;27:5708–5714. [PubMed: 16901540]
39. Brewster L, Brey EM, Addis M, Xue L, Husak V, Ellinger J, et al. Improving endothelial healing with novel chimeric mitogens. Am J Surg 2006;192:589–593. [PubMed: 17071189]
40. Gajdusek C, Carbon S, Ross R, Nawroth P, Stern D. Activation of coagulation releases endothelial cell mitogens. J Cell Biol 1986;103:419–428. [PubMed: 3733873]
41. Grieb TA, Burgess WH. The mitogenic activity of fibroblast growth factor-1 correlates with its internalization and limited proteolytic processing. J Cell Physiol 2000;184:171–182. [PubMed: 10867641]
42. Wiedlocha A, Falnes PO, Madshus IH, Sandvig K, Olsnes S. Dual mode of signal transduction by externally added acidic fibroblast growth factor. Cell 1994;76:1039–1051. [PubMed: 7511061]
43. Brewster LP, Bufallino D, Ucuzian A, Greisler HP. Growing A Living Blood Vessel: insights for the second hundred years. Biomaterials. 2007In Press
44. Haudenschild CC, Schwartz SM. Endothelial regeneration. II. Restitution of endothelial continuity. Lab Invest 1979;41:407–418. [PubMed: 502473]
45. Reidy MA, Clowes AW, Schwartz SM. Endothelial regeneration. V. Inhibition of endothelial regrowth in arteries of rat and rabbit. Lab Invest 1983;49:569–575. [PubMed: 6632774]
46. Greisler HP, Cziperle DJ, Kim DU, Garfield JD, Petsikas D, Murchan PM, et al. Enhanced endothelialization of expanded polytetrafluoroethylene grafts by fibroblast growth factor type 1 pretreatment. Surgery 1992;112:244–254. [PubMed: 1641764]discussion 254–245
47. Cao H, Dronadula N, Rao GN. Thrombin induces expression of FGF-2 via activation of PI3K-Akt-Fra-1 signaling axis leading to DNA synthesis and motility in vascular smooth muscle cells. Am J Physiol Cell Physiol 2006;290:C172–182. [PubMed: 16148030]

48. Sturge J, Carey N, Davies AH, Powell JT. Fibrin monomer and fibrinopeptide B act additively to increase DNA synthesis in smooth muscle cells cultured from human saphenous vein. J Vasc Surg 2001;33:847–853. [PubMed: 11296341]

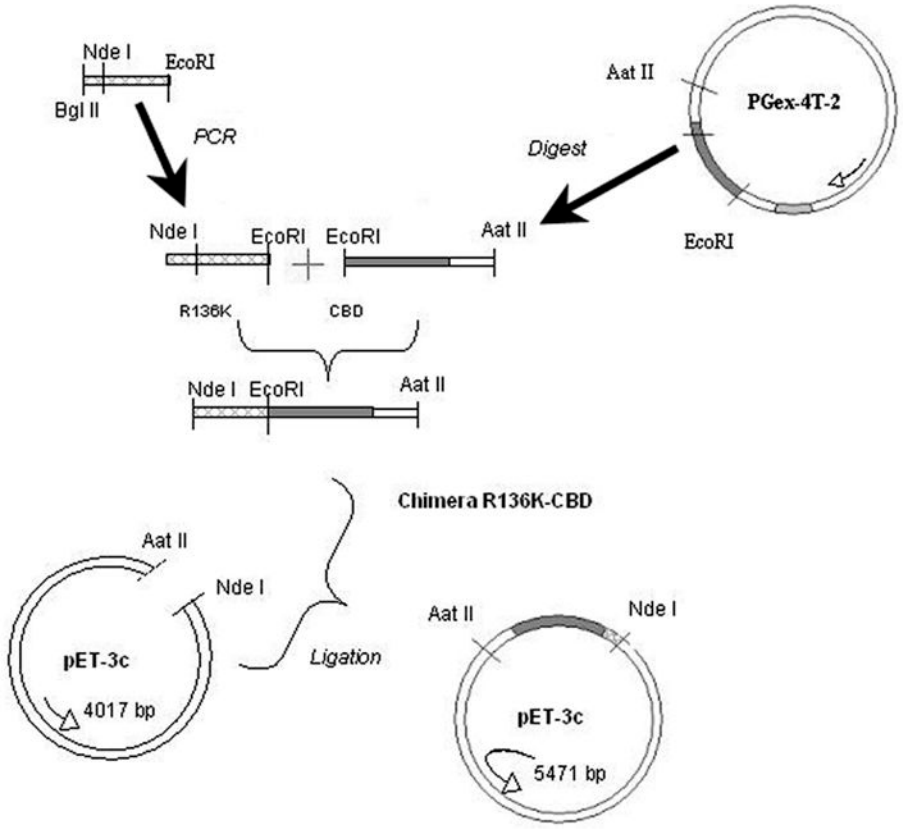

Figure 1.
Schema of R136K-CBD Generation

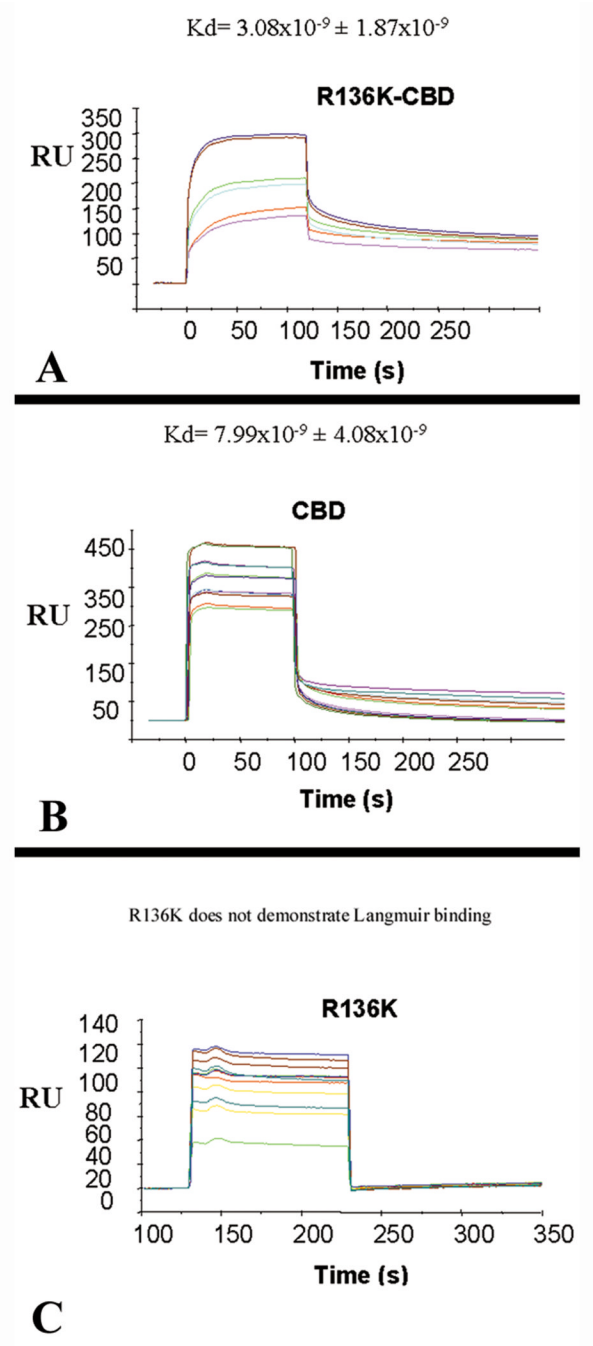

Figure 2. R136K-CBD exhibits Langmuir binding to collagen

a–c. At 100, 200, and 400 nmol/L, BIAcore analysis of R136K-CBD (a) and CBD (b) demonstrated Langmuir binding with similar dissociation constants, while R136K did not (c).

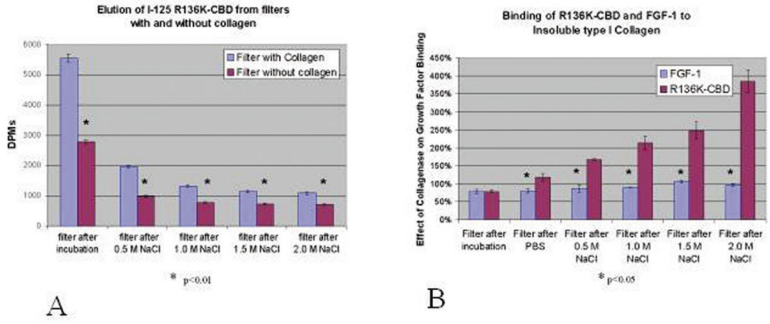

Figure 3. R136K-CBD binds to collagen avidly and selectively

a. Binding of ^{125}I-R136K-CBD to collagen in Millipore filter system was significantly greater than binding to filter system itself after initial incubation and all subsequent salt elutions. b.^{125}I-R136K-CBD, but not ^{125}I-FGF-1, binds selectively to intact collagen as compared to collagenase-degraded collagen; this is signified on the Y-axis by a percentage ratio >100%, i.e. more binding to intact collagen than collagenase-degraded collagen. Although significantly greater with ^{125}I-R136K-CBD after an initial washing with PBS, this difference becomes more prominent with each increasingly stringent salt elution (366% at 2 mol/L NaCl).

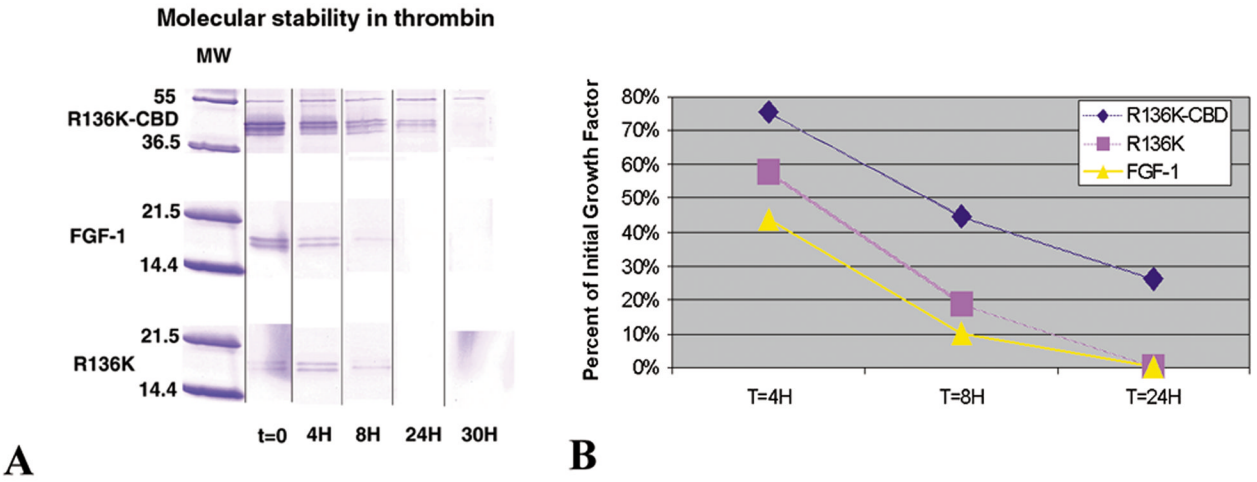

Figure 4. R136K-CBD is resistant to thrombin degradation

a. To determine the effect of ligating the CBD to R136K on its molecular integrity, R136K-CBD was incubated with thrombin for 30 hours. A representative gel demonstrates the band density of R136K-CBD (Mr 41kDa), FGF-1 (Mr 17kDa), and R136K (Mr 17kDa). Lanes 3,4 and 5 illustrate the decrease in band intensity bands over time for both FGF-1 and R136K as compared to R136K-CBD.

b. This was quantified by densitometry where R136K-CBD's integrity as a function of degradation over time was superior to both FGF-1 and R136K.

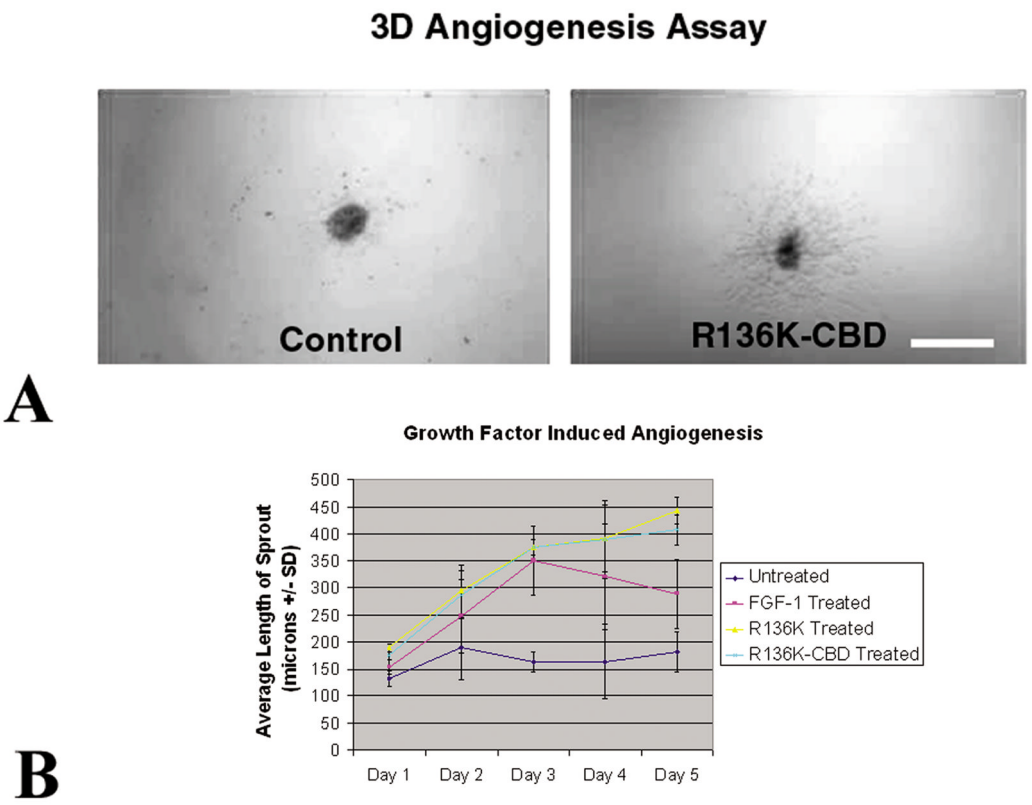

Figure 5. R136K-CBD demonstrates prolonged angiogenic activity

a. Representative image from our angiogenesis assay at day 5 comparing R136K-CBD treated ECs with an untreated control (normal saline without growth factor). Bar scale represents 500μ.

b. Mean average sprout length ± SD with growth factor stimulation over 5 days. Here R136K and R136K-CBD, but not FGF-1, demonstrate sustained angiogenic activity while embedded in a 3-D fibrin glue matrix; this was significantly greater than untreated HUVECs out to 5 days (P=.002). All growth factors were significantly greater than the untreated group at 3 days (P<. 0001), but the FGF-1-treated group began to have sprout regression evident by day 4.

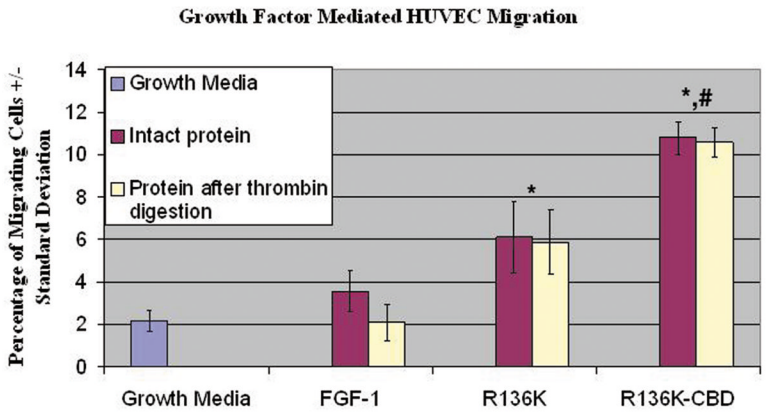

Figure 6. R136K-CBD is a thrombin-resistant chemotaxin for HUVECs

R136K-CBD was significantly greater than that of R136K (#), and both R136K and R136K-CBD demonstrated greater chemotactic activity than FGF-1 (*). Thrombin pre-treatment did not affect R136K-CBD or R136K activity. However FGF-1's chemotactic activity was abrogated by thrombin incubation.

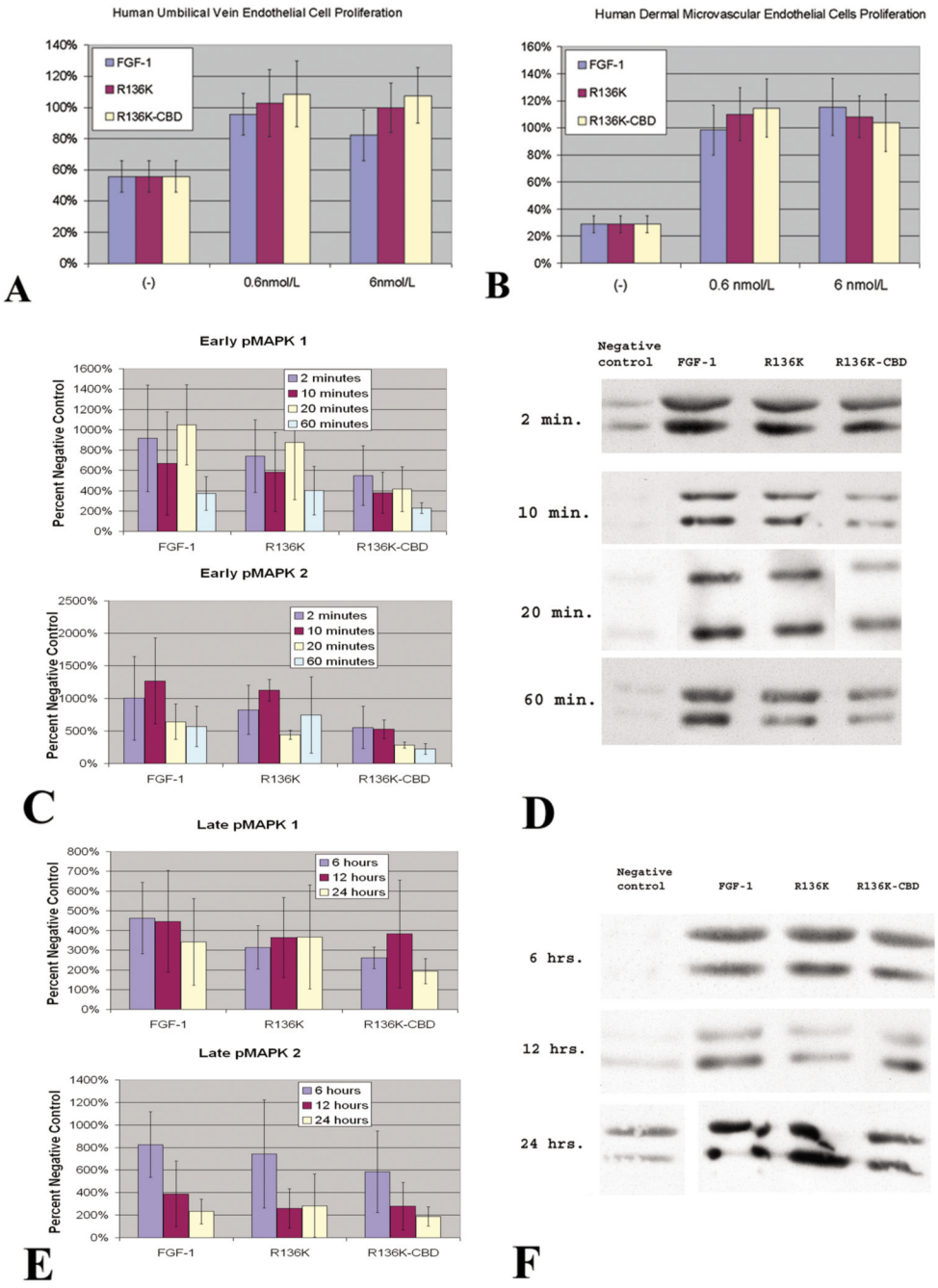

Figure 7. R136K-CBD retains FGF-1's mitogenicity in human ECs

a–b. Mitogenic activity of growth factors expressed as percent positive control (20% FBS) and compared to negative control (20% PBS). R136K-CBD stimulates HUVEC (a) and HMEC (b) proliferation to a similar degree as FGF-1 and R136K beginning at 0.6 nmol/L, and all of the growth factors demonstrate mitogenic activity similar to positive control and significantly greater than negative control.

c–d. Early pMAPK 1 and 2 activation compared to negative control. Bar graph shows mean pMAPK 1 and 2 levels ± SD at various time points up to 60 minutes. Representative Western blots from HUVEC lysates demonstrate relative increase in pMAPK 1 (top:44kDa) and 2 (bottom:42kDa) levels compared to negative control.

e–f. Late pMAPK 1 and 2 activation compared to negative control. Bar graph shows mean pMAPK 1 and 2 levels ± SD at selected time points up to 24 hours after growth factor stimulation. Representative Western blots from HUVEC lysates demonstrate persistently increased pMAPK 1 and 2 levels compared to negative control out to 24 hours.